

BURIED PIPELINES SUBJECTED TO GROUND DEFORMATION CAUSED BY LANDSLIDE TRIGGERING

Angelos Tsatsis¹, Rallis Kourkoulis¹ and George Gazetas¹

¹ National Technical University of Athens
Heroon Polytechniou 9, Athens, Greece
ag_tsa@yahoo.gr, rallisko@sgm-engineering.com, gazetas@ath.forthnet.gr

Keywords: Pipelines, Landslide, Permanent Ground Deformation, Soil-Structure Interaction, Geotechnical Earthquake Engineering.

Abstract. *Permanent ground deformation is one of the most damaging hazards for buried lifelines such as gas and oil pipelines. The most frequent cause of permanent ground deformation is a landslide. Landslides can be triggered by a variety of causes, yet the factors responsible for the most damaging landslides are water and especially earthquake. The scope of this study is to investigate the response of a continuous buried pipeline subjected to ground deformation caused by landslide triggering, considering two characteristic cases: (a) the pipeline running perpendicularly to the soil movement vector and (b) the pipeline is parallel to the soil movement vector. An idealized landslide of 3D geometry is considered. Due to the inconsistency between the colossal dimensions of the landslide and the much smaller pipe geometry (a combination that would call for a numerical model of several millions elements), the problem is decoupled. In the first step, a “global” free-field model is employed to simulate the landslide evolution, ignoring the presence of the pipeline. The free field analysis provides the input for the second step, in which a “local” detailed model of the pipeline, along with the surrounding soil, is used to simulate its distress. This allows the use of adequately large elements for the global model, and reasonably small elements for the local one, circumventing the aforementioned scale-related problem.*

1 INTRODUCTION

Oil and gas pipelines typically run for very long distances (of the order of hundreds or even thousand kilometers) crossing various topographic anomalies such as slopes. Many of these slopes can be prone to failure during an earthquake or heavy precipitation incident and therefore potentially hazardous for landsliding occurrence. Past experience has proved that pipelines are quite vulnerable to permanent ground deformation (such as landslide) compared to other geohazards such wave propagation [1] [2]. Therefore, it is of paramount importance to be able to realistically simulate the response of pipelines subjected to ground deformation caused by landslide triggering. To this end, this study presents an integrated numerical methodology for the simulation of both the landslide triggering and evolution as well as the response of the pipeline that crosses the critical area.

2 ANALYSIS METHODOLOGY

The 3D nature of the problem is accounted for and the simulation is conducted in 3D. Since the simultaneous simulation of the pipe and the landslide is practically impossible the problem is decoupled. This happens because in order to simulate pipe instability issues, such as local buckling, a very fine mesh is needed for the pipe and the soil at its vicinity. On the other hand, this demand cannot be combined with the large dimensions of the landslide. According to the decoupled methodology, the landslide evolution is first analyzed ignoring the presence of the pipe assuming that the presence of the pipe does not affect the landslide at a global level. The free field analysis provides the input for the second step, in which a “local” detailed model of the pipeline, along with the surrounding soil, is used to simulate its distress. This allows using adequately large elements for the global model, and reasonably small elements for the local one, circumventing the aforementioned scale-related problem.

3 NUMERICAL SIMULATION OF THE LANDSLIDE

Landslides can be of various types. The most widely used classification system was devised by Varnes [3]. Varnes identified five principal categories: falls, topples, slides, spreads, and flows. With respect to the distress of the pipeline, falls and topples may cause damage to above-ground pipelines by direct impact of falling rocks. These types of landslide have little effect on buried pipelines though given that the embedment depth is adequate. In cases of spreads and flows the transported material behaves as a viscous fluid, for which the properties must be defined with caution. On the other hand, in an earth slide, the soil moves more or less as a block, with the materials retaining approximately the same properties with their initial state. For the purposes of this study, an idealized rotational slide is considered. The geometry of the slope and the properties of the soil remain constant. A distinct zone of weakness is pre-defined, representing the interface between the stable “healthy” soil and the unstable part of the slope, consisting of a loose material (a hypothesis of deposits from a previously triggered landslide is made).

A section of the analyzed slope is presented in Figure 1a (i.e., the two dimensional geometry of the landslide). The elevation difference between the foot and the crest of the slope is 20 m, while the length of the slope is 70 m, yielding a slope angle of 16° . Regarding the sliding surface geometry, a circular failure surface is assumed, described by the intersection of the slope with a circle of radius $R = 100$ m, with its center 95 m higher and 15 m to the left of the toe of the slope foot. In order to obtain the 3D geometry of the landslide, it is tactically assumed that the 2D section of Figure 1 corresponds to the middle cross section of the landslide, where the largest volume of material is mobilized, while the sliding surface is getting shallower as it moves away from the middle cross section. The 3D geometry of the sliding soil

mass is introduced through the intersection of the 3D slope with the cutting shape that is presented in Figure 1b. This cutting shape comprises a circular middle section in the z - x plane, identical to that presented above. However, in both x - y and y - z plane the adopted shape comprises elliptical sections in order to simulate a smooth sliding mass shape fade out.

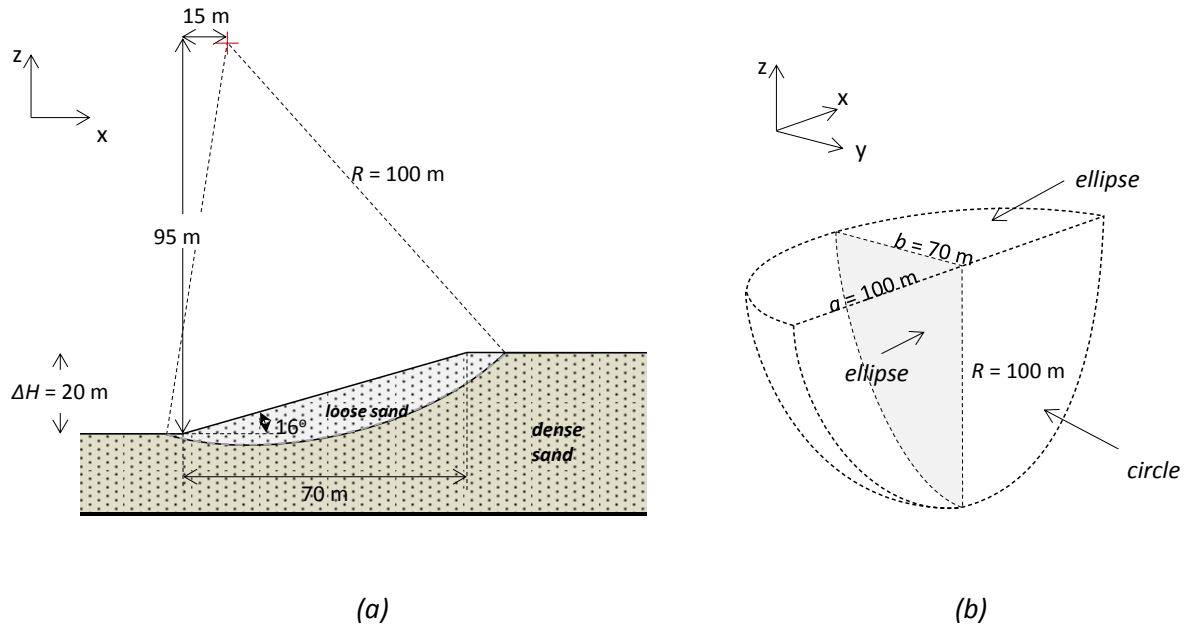


Figure 1: (a) The 2D geometry of the slope and the selected circular cutting plane and (b) the cutting shape used to derive the 3D geometry.

In Figure 2 the finite element model used is briefly presented. Taking advantage of the symmetry of the problem geometry, half of the slope is examined. The middle section, where the largest volume of material is mobilized, is the surface of symmetry. The sliding mass is assumed to consist of a loose material and therefore simulated with a loose sand of Young's modulus $E = 10$ MPa and friction angle $\varphi = 32^\circ$. The stable soil surrounding the sliding mass comprises dense sand of $E = 25$ MPa and $\varphi = 45^\circ$. The soil is modeled with 8-noded brick type elements, while its strength and nonlinear response is described with a Mohr-Coulomb constitutive model. The sliding plane is simulated with a row of elements of reduced stiffness and strength ($E = 8$ MPa and $\varphi = 30^\circ$) between the sliding mass and the stable soil. The landslide is triggered by progressively reducing the strength of these elements with time from $\varphi = 30^\circ$ to $\varphi_{res} = 5^\circ$.

Figure 3 presents snapshots of the triggering and evolution of the landslide. As expected, due to the 3D depiction of the geometry of the slide, the soil does not dislocate in a uniform manner throughout the sliding mass; both displacement magnitude as well as the vector of the displacement vary along the sliding mass. It is worth noting that for this slope, the landslide triggering takes place near the crest of the slope, since the inclination of the failure surface is larger in this area. As observed from the displacement contours, during the initial stages of the phenomenon, the soil near the crest of the slope displaces significantly more than the soil near the toe of the slope (top right snapshot). Subsequently, there comes a point where the landslide fully mobilizes and the displacement of the sliding mass becomes more uniform (bottom left snapshot for maximum displacement $U = 1$ m). In the ensuing the displacement of the point lying on the crest line and on the plane of symmetry (called hereon reference point) is used as an index to describe the evolution of the landslide.

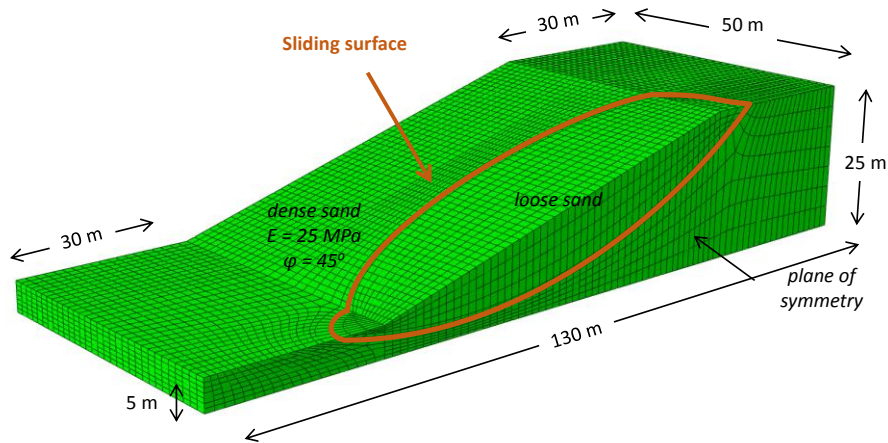


Figure 2: The finite element model of the landslide.

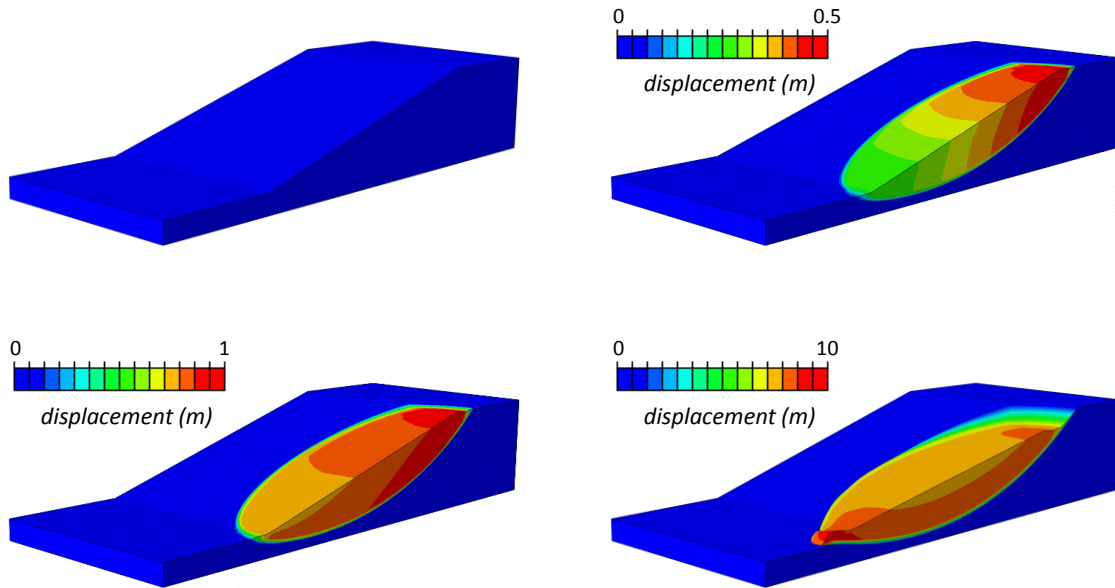


Figure 3: Representative snapshots of the landslide evolution.

4 PIPELINE – LANDSLIDE INTERACTION

A continuous steel pipeline is considered that crosses the aforementioned slope. Two extreme cases are investigated: (a) the pipeline crosses perpendicularly the slope and the potential soil movement direction is parallel to its axis and (b) the pipeline runs in parallel with the slope contour lines and the soil movement direction is perpendicular to its axis. The pipe is made of X65 steel with yield stress $\sigma_y = 450$ MPa and maximum stress $\sigma_{max} = 545$ MPa at strain $\varepsilon_{max} = 0.2$. The pipe is of diameter $D = 36''$ and it is designed for a maximum internal pressure of $p_{max} = 9$ MPa. Its thickness is calculated at $t = 12.7$ mm as dictated by the expression:

$$p_{max} = 0.72 * \left(\frac{2\sigma_y t}{D} \right) \quad (1)$$

To make the results more realistic the pipeline is considered to be functional under operating pressure $p_{oper} = 6$ MPa. The pipe is assumed to be embedded in depth 1.5 m from the surface to the crown pipe.

4.1 Pipeline axis parallel to the soil movement

To begin with, the case where the pipe axis is normal to the contour lines of the slope is considered. The centerline of the pipe is at 2 m away from the plane of symmetry of the slope. In order to accommodate the change in the axis inclination two bends are used, one at the toe and one at the crown of the slope. Those bends have a radius of curvature 40 times the pipe diameter (representative of cold bends).

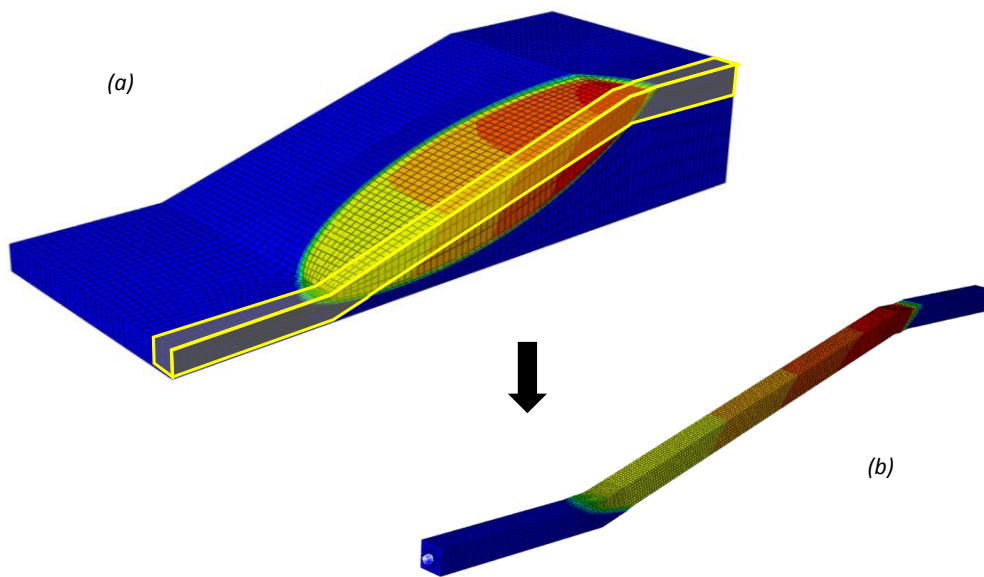


Figure 4: The displacement time histories are extracted from the “global” free field model and imposed as input at the boundaries of the “local” pipeline - soil interaction model.

After the installation of the pipe the aforementioned landslide occurs. As already stated, the analysis is decoupled (Figure 4). Figure 5 presents the local finite element model, used to model soil–pipeline interaction and its various components. Only a soil prism around the pipe is modeled. The pipeline is modeled with 4-noded reduced integration shell elements. 48 elements along the pipe circumference are used of length $d_{FE} = 2.5$ cm, aiming to realistically capture local instability phenomena.

For the correct simulation of the pipe response, the behavior of the pipe beyond the boundaries of the 3D model has to be accounted for. The soil displacement is expected to cause (among others) axial stressing to the pipe. Axial distress may affect large length of the pipe (of the order of several hundred meters or even kilometers), rather than the limited segment that is simulated in this analysis. In order to account for the axial response of the pipe along its theoretically infinite length the following procedure is followed. First, the soil reaction to axial pulling of the pipe is calculated. For this, a full 3D finite element model of a pipe segment within the soil is employed. The model accounts for the inelastic behavior of the soil and the contact between the pipe and the soil considering interface friction (in this case friction coefficient between the pipe and the surrounding soil is $\mu = 0.5$). The pipe is considered rigid. Knowing the soil reaction per meter to a potential axial movement of the pipe, a simpli-

fied model is used to calculate the force – displacement response of the soil pipe system to an imposed axial displacement. This simplified model is lengthy enough to be considered infinite (the stresses developed on the pipe dissipate within the length simulated). The soil reaction is simulated with distributed springs along the pipe length that are calibrated against the force-displacement behavior of the soil derived from the first step. The pipe is simulated with beam elements accounting for the steel material nonlinearity. An axial displacement is applied at the end of the pipe and the reaction of the pipe–soil system is measured. This reaction (in terms of force – displacement) is attributed to a nonlinear spring at the ends of the pipe at the boundaries of the 3D pipe – landslide interaction model.

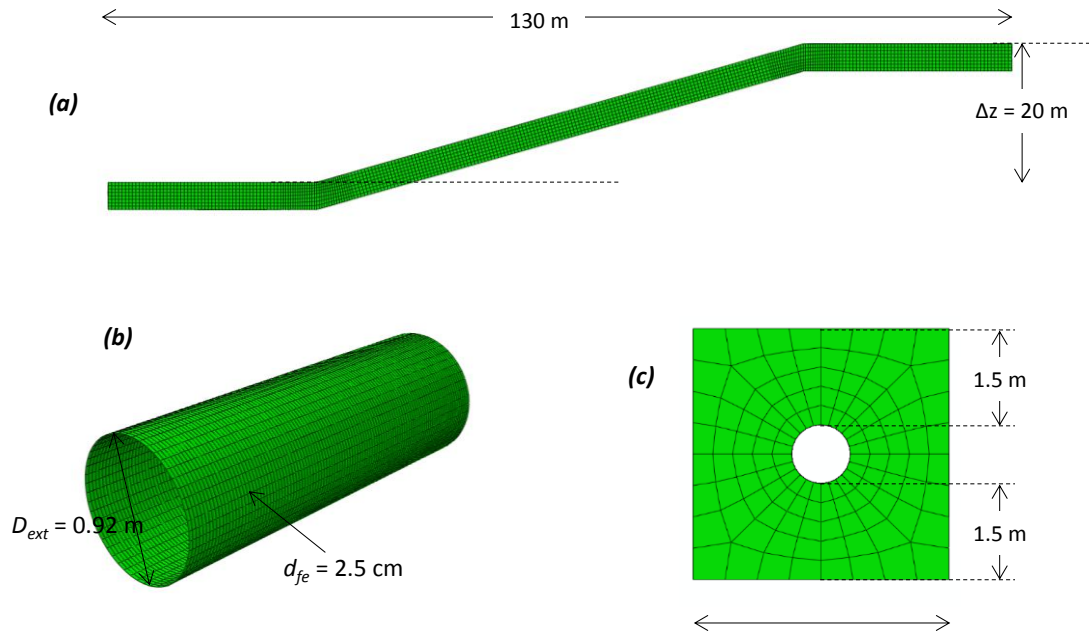


Figure 5: The finite element model that focuses on the soil–pipeline interaction for the case of pipeline positioned parallel to the soil movement: (a) longitudinal view of the model, (b) a detailed view of the pipeline mesh, (c) Cross section showing the meshing of the soil and the dimensions of the soil prism.

Figure 6 presents the deformed mesh of the pipe–landslide interaction model corresponding to displacement magnitude of the reference point $U_{ref} = 0.75$ m. Figure 6a presents the deformed mesh of the soil prism with superimposed displacement contours, while Figure 6b presents the deformed mesh of the pipe with superimposed stress contours. It is proven that the two bends are the most stressed components by the downslope movement of the soil. Figure 6c concentrates on the top bend (i.e. the one at the crown of the slope). The stressing mechanism can be seen as mechanically analogous to a normal fault. The failure surface where the sliding of the soil mass occurs can be seen as the rupture. Therefore, a part of the bend is fixed within the stable soil while the rest is dragged downwards and outwards by the moving soil. The fixed part bends as cantilever developing tension at the top side and compression at the bottom side, while the dislocating part develops compression at the top side and tension at the bottom side. The bottom bend exhibits similar response, only this time the response mechanism is analogous to a reverse fault. Due to the geometry of the sliding surface, at the intersection with the pipe at the vicinity of the slope toe the soil goes upwards with the simultaneous compression component. The part of the pipe that follows the sliding mass is stressed by the underlying soil (bending) resulting in compression at the bottom side and tension at the top side of the pipe. The part of the pipe that lies within the stable soil bends due to reactions from the overlying soil with the top side under compression and the bottom side un-

der tension. Yet, the downward movement of the soil prevails with the pipe ultimately failing due to local buckling at the part of the bend that is within the stable soil.

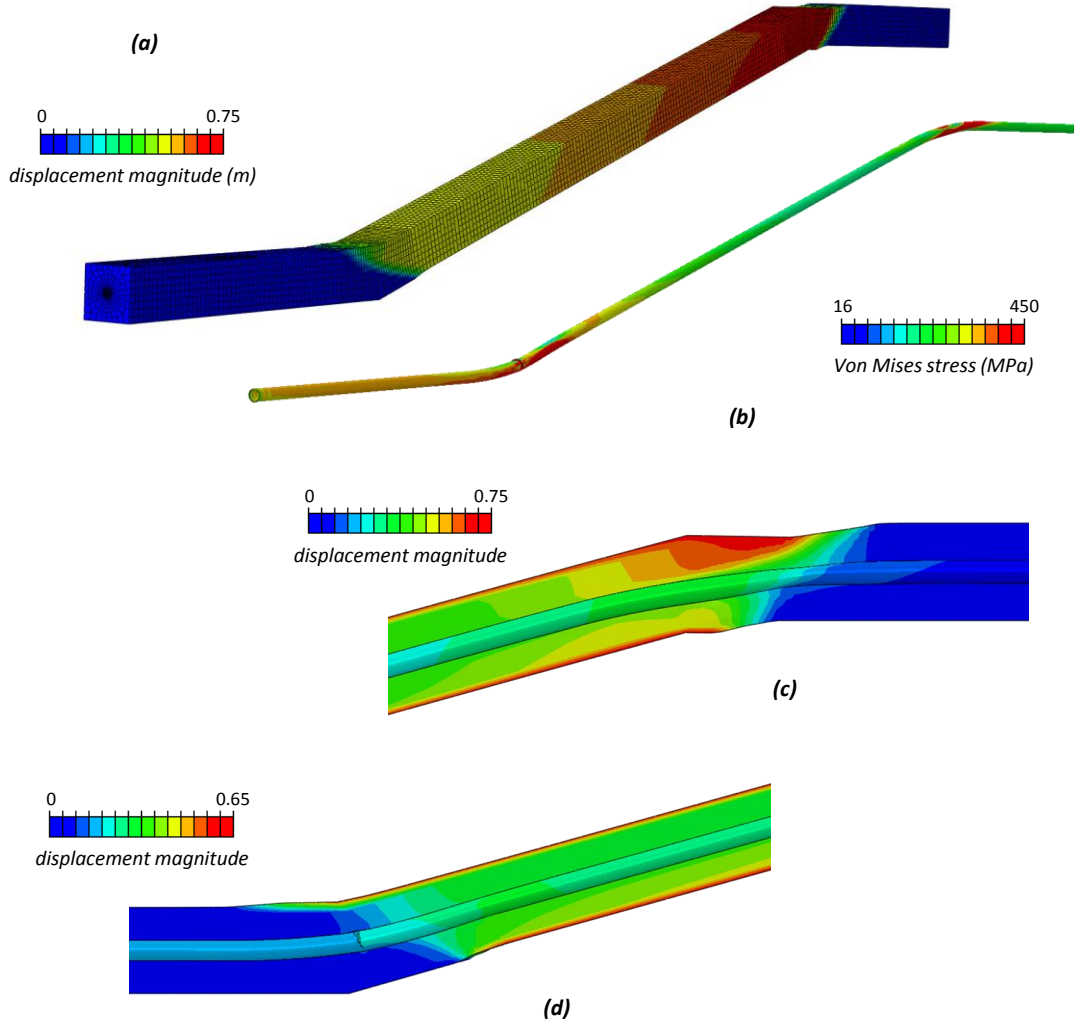


Figure 6: Deformed mesh of the pipeline – landslide interaction problem for displacement magnitude of the reference point $U_{ref} = 0.75$ m. (a) Deformed mesh of the soil prism. (b) Deformed mesh of the pipe. (c) Cross section of the deformed model concentrating on the top bend. (d) Cross section of the deformed model concentrating on the bottom bend.

Figure 7 and Figure 8 present a closer look at the response of the two bends. Figure 7a presents the deformed mesh of the top bend with superimposed axial strain contours depicting the response mechanism described above. Figure 7b presents the axial strain distribution along the tensile side of the critical area. Considering a tensile failure criterion of $\varepsilon_{max} = 3\%$ [3], the pipe ultimately fails for $U_{ref} = 0.46$ m of displacement of the reference point. Figure 8a presents the deformed mesh of the bottom bend with superimposed axial strain contours, while in Figure 8b the axial strain distribution along the compressive side of the critical area of the bottom bend is presented. As evidenced by the shape of the distribution, wrinkling occurs for displacement of the reference point (at the slope crest) $U_{ref} = 51$ cm. Practically, the two bends fail at the same time, with a minor difference in the critical displacement of the reference point (51 cm for the bottom bend compared to 46 cm for the top bend). However, we

have to remind that this displacement is not uniform throughout the sliding mass; when the reference point at the crest line of the slope has been displaced by 51 cm the respective point at the toe line has displaced 28 cm.

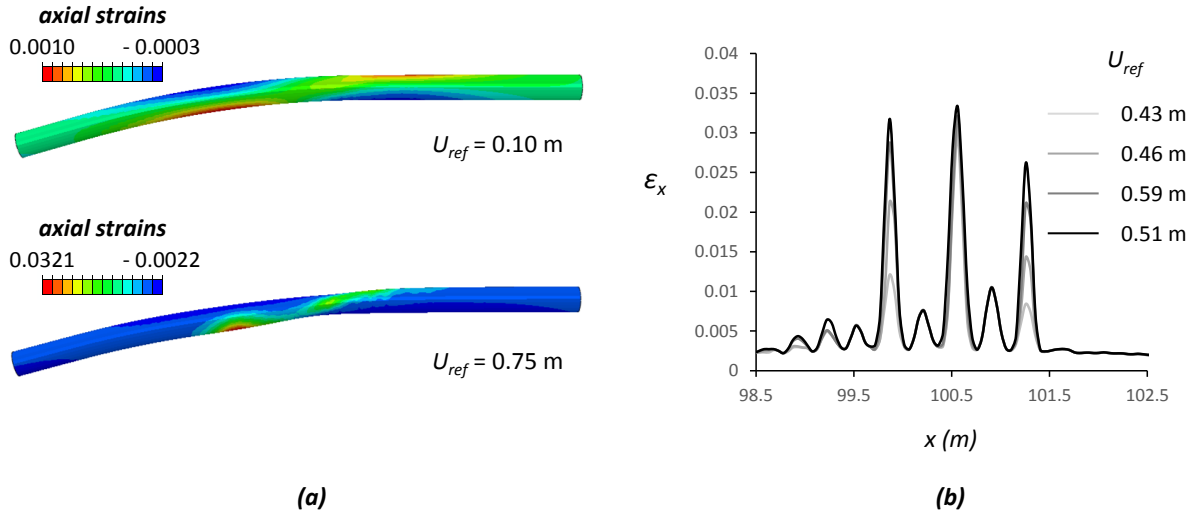


Figure 7: The finite element model that focuses on the soil–pipeline interaction for the case of pipeline positioned parallel to the soil movement: (a) longitudinal view of the model, (b) a detailed view of the pipeline mesh, (c) Cross section showing the meshing of the soil and the dimensions of the soil prism.

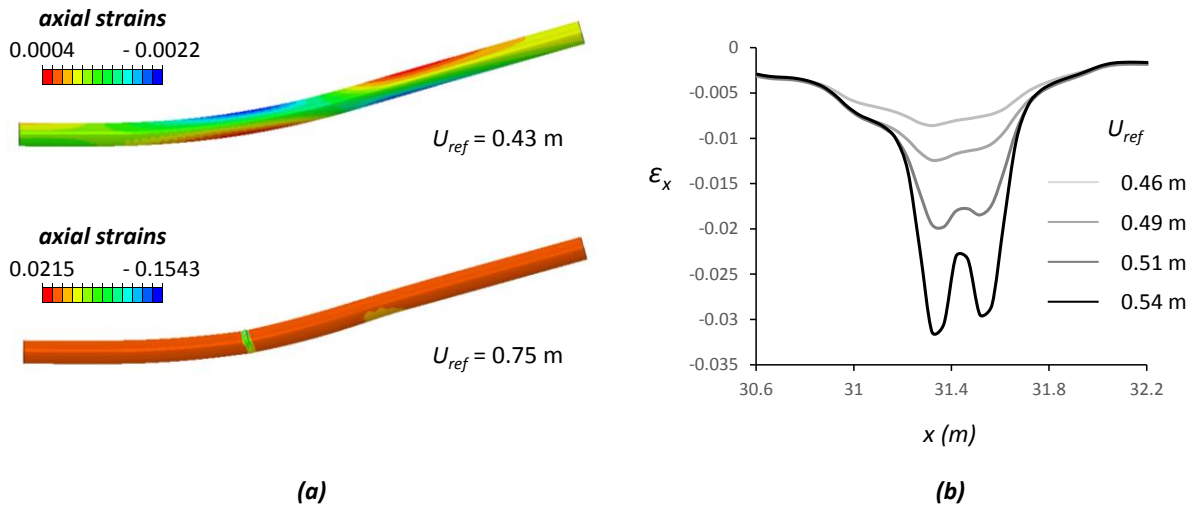


Figure 8: The finite element model that focuses on the soil–pipeline interaction for the case of pipeline positioned parallel to the soil movement: (a) longitudinal view of the model, (b) a detailed view of the pipeline mesh, (c) Cross section showing the meshing of the soil and the dimensions of the soil prism.

4.2 Pipeline axis perpendicular to the soil movement

In this section, the other extreme case is considered where the pipe runs in parallel with the contour lines of the slope intersecting at 90° with the potentially unstable soil deposit. As an illustrative example of such case, the pipe axis is assumed to be located at the middle of the slope between the toe and the crest of the slope. As explained before, in order to analyze the response of the pipeline subjected to the landslide actions the problem is decoupled. The free

field analysis provides the input for the second step, in which a “local” detailed model of the pipeline, along with the surrounding soil, is used to simulate its distress as shown in Figure 9.

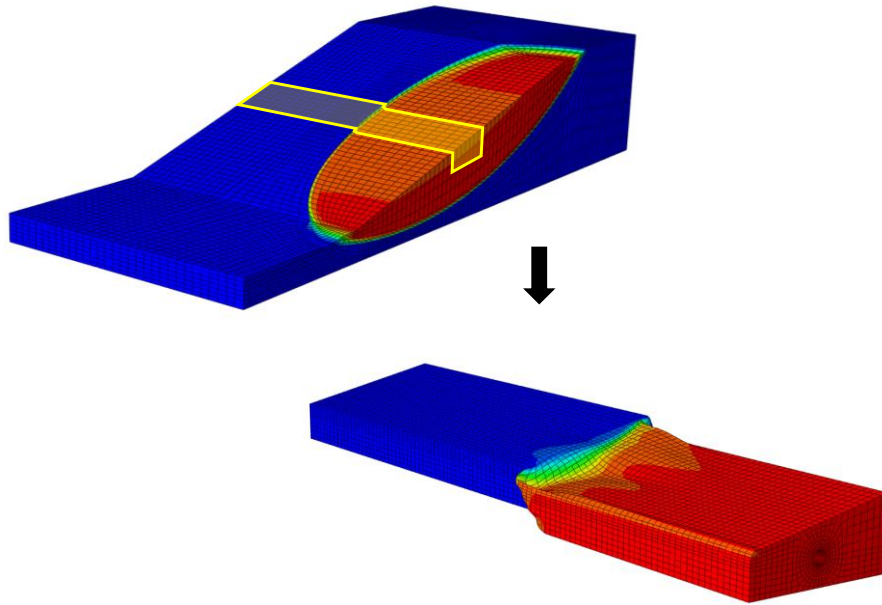


Figure 9: The finite element model that focuses on the soil–pipeline interaction for the case of pipeline positioned parallel to the soil movement: (a) longitudinal view of the model, (b) a detailed view of the pipeline mesh, (c) Cross section showing the meshing of the soil and the dimensions of the soil prism.

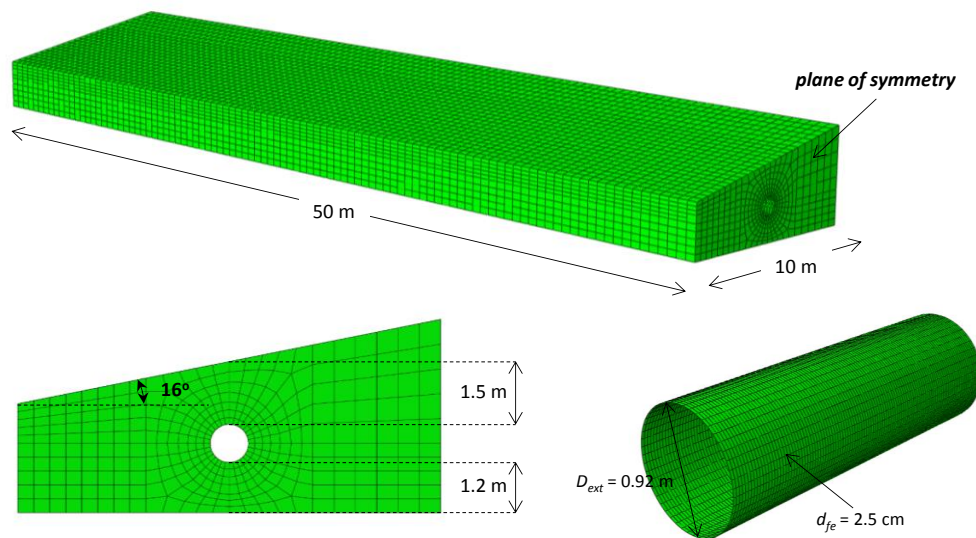


Figure 10: The finite element model that focuses on the soil–pipeline interaction for the case of pipeline positioned perpendicular to the soil movement: the dimensions of the soil prism, a cross section of the prism and a detail of the pipeline mesh.

The finite element model that focuses on the pipeline – landslide interaction is presented in Figure 10. As with the free field model, taking advantage of the symmetry of the problem only half of the pipeline is modeled. In the plane of symmetry all the appropriate degrees of

freedom are constrained. On the other end of the 3D model the pipeline – soil behavior is taken into account using nonlinear springs. The displacements calculated from the free field analysis are imposed at the bottom of the model and at the two sides parallel with pipe axis. Therefore, the distance of these two sides from the pipe axis is equal to 5 diameters to minimize any boundary effects, and to allow any interaction phenomena between the pipe and the surrounding soil to take place.

Figure 11 presents the deformed mesh of the pipe – landslide interaction model for displacement magnitude of the reference point $U_{ref} = 1.07$ m. It should be noted that at this specific moment, the soil that lies on the plane of symmetry at the immediate vicinity of the pipe (and therefore the pipe end at the plane of symmetry) has been displaced $U = 0.95$ m. The pipe deforms due to the landslide induced actions and axial strains are developed as shown in for the same Figure 11b displacement. Two maximum curvature points are observed, where the concentration of the axial strains is substantial. The pipe ultimately fails due to excessive tensile strains at the tensile side of the maximum curvature point within the stable soil (Figure 11c). This is expected since the stable soil is of greater strength than the sliding soil, resulting in increased actions on the pipe. Finally, Figure 11d presents the evolution of the axial strain distribution along the most stressed generator at the critical area. Considering a failure criterion of maximum tensile axial strain $\varepsilon_{max} = 3\%$ the pipe fails for displacement magnitude of the reference point $U_{ref} = 1.0$ m (which translated to 0.89 m of displacement of the pipe end lying on the plane of symmetry).

5 CONCLUSIONS

In this study, a two-step analysis methodology has been developed, allowing realistic simulation of pipeline distress due to landslide displacement. Landslides have a 3D geometry, which depends on a variety of factors, which are quite unique for each case. In terms of an illustrative example, an idealized landslide was selected and analyzed. To overcome numerical difficulties, arising from the scale differences between the landslide and the pipeline, the problem is decoupled and the analysis is conducted in two steps. In the first step, a global free-field model is used to simulate the evolution of the landslide, ignoring the presence of the pipeline. In the second step, a more detailed local model is developed, comprising the pipeline and the surrounding soil. The computed displacement time histories from the first step (global model) are imposed as boundary conditions to the local model. The methodology was employed for an illustrative example. A 36'' pipeline of thickness $t = 12.7$ mm and internal pressure of 6 MPa crosses an idealized rotational landslide considering two characteristic cases: one where the pipeline axis is parallel to the soil movement and one where it is perpendicular to the soil movement. In the first case the bends prove to be most vulnerable components and the pipeline fails for $U_{ref} = 0.46$ m of displacement of the reference point. In the second case the pipe fails for $U_{ref} = 1$ m of displacement of the reference point.

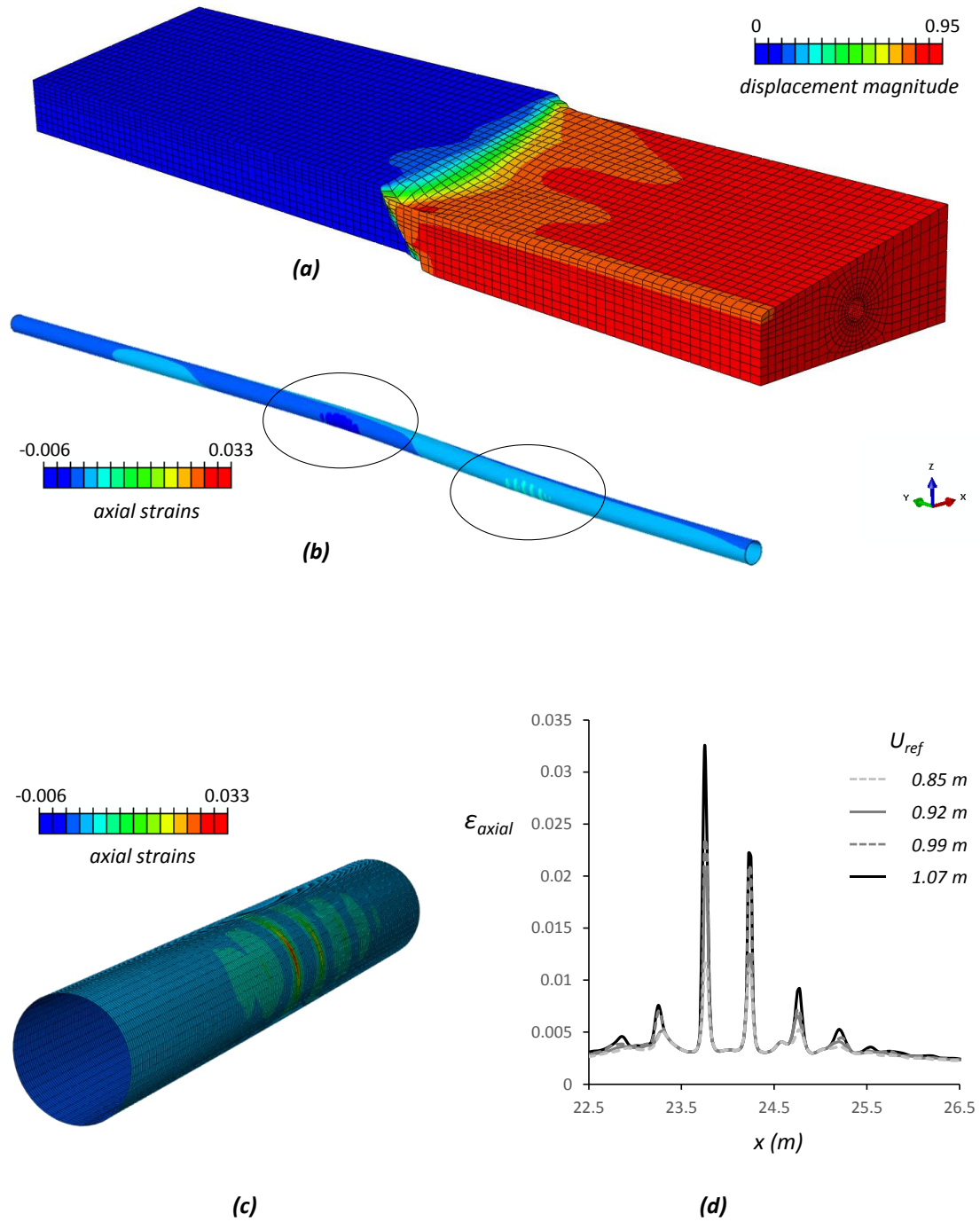


Figure 11: (a) The deformed mesh of the pipeline – landslide interaction model with superimposed displacement contours for displacement of reference point $U_{ref} = 1.07$ m. (b) Deformed pipe with superimposed axial strain contours for the same displacement. (c) Detail of the pipe mesh at the area of the maximum curvature point within the stable soil (critical area). (d) Evolution of the axial strains at the most stressed generator of the critical area of the pipe with the increase of the pipe displacement.

ACKNOWLEDGEMENT

This research has been co-financed by the European Union (European Social Fund – ESF) and Greek national funds through the Operational Program "Education and Lifelong Learning" of the National Strategic Reference Framework (NSRF) – Research Funding Program: Thales. Investing in knowledge society through the European Social Fund, Project ID "UPGRADE".

REFERENCES

- [1] Ariman T, Muleski GE. A review of the response of buried pipelines under seismic excitations. *Earthquake Engineering and Structural Dynamics* 1981;9:133-51
- [2] Liang J, Sun S. Site effects on seismic behaviour of pipelines: a review. *ASME Journal of Pressure Vessel Technology* 2000;122(4):469-75.
- [3] EN 1998-4 (1993). "Eurocode 8: Design of structures for earthquake resistance. Part 4: Silos, Tanks and Pipelines", CEN, Brussels.